TENT: Tensorized Encoder Transformer for temperature forecasting

Onur Bilgin*, Paweł Mąka*, Thomas Vergutz*, Siamak Mehrkanoon**

Department of Data Science and Knowledge Engineering, Maastricht University, The Netherlands

Abstract

Reliable weather forecasting is of great importance in science, business and society. The best performing data-driven models for weather prediction tasks rely on recurrent or convolutional neural networks, where some of which incorporate attention mechanisms. In this work, we introduce a new model based on the Transformer architecture for weather forecasting. The proposed Tensorial Encoder Transformer (TENT) model is equipped with tensorial attention and thus it exploits the spatiotemporal structure of weather data by processing it in multidimensional tensorial format. We show that compared to the encoder part of the original transformer and 3D convolutional neural networks, the proposed TENT model can better model the underlying complex pattern of weather data for the studied temperature prediction task. Experiments on two real-life weather datasets are performed. The datasets consist of historical measurements from USA, Canada and European cities. The first dataset contains hourly measurements of weather attributes for 30 cities in USA and Canada from October 2012 to November 2017. The second dataset contains daily measurements of weather attributes of 18 cities across Europe from May 2005 to April 2020. We use attention scores calculated from our attention mechanism to shed light on the decision-making process of our model and have insight knowledge on the most important cities for the task.

Keywords: Weather forecasting, tensorial input, tensorial attention mechanism, tensorized transformer, temperature prediction

1. Introduction

In various application domains one often encounters multivariate time series data, such as stock market prices, road traffic flows, or weather conditions in different cities, to name a few [1]. Predicting new trends and patterns in time series domains based on historical observations is the focus of many research efforts. In particular, in the last decade, data-driven based models have shown promising results in weather forecasting applications.

Reliable weather forecasting constitutes a challenge that is of great scientific, economic and social significance. Changing weather conditions impact many aspects of life, ranging from catastrophe and disaster management to many economic sectors, including transport, agriculture, energy generation, among others [2]. The undergoing energy transformation to renewable energy production is only one of many sources of increasing demand for estimates of future weather conditions such as air temperature or wind speed [3]. High quality temperature and wind forecasts increase the precision of estimates of future energy generation through wind and solar power [3]. Even a small increase in the prediction precision can have significant implications for the maximization of power generation [4] or the planning of energy distribution and power plant dispatching [3].

This paper focuses on temperature forecasting task. In particular, here we present three contributions. First, a transformer architecture for tensorial input equipped with a new self-attention mechanism for analyzing 3D tensor data inputs is introduced. Second, the comparison of the new algorithm to encoder part of the original transformer and 3D convolutional neural network algorithms for temperature prediction task is given. Third, the explainability of the tensorial attention algorithm using data visualization tools is provided.

This paper is structured as follows. A review of related work for weather forecasting is given in section 2. Our tensorial self-attention and transformer architecture for tensorial input are introduced in section 3. The datasets for the evaluation of the models and the obtained results are reported in section 4. In section 5 the experimental results and the analysis of the tensorial-attention are given. We drew our conclusions in section 6.

2. Related Work

2.1. Weather forecasting

Conventionally, weather forecasting is done by using Numerical Weather Prediction (NWP). NWP uses mathematical models to describe physical processes and weather conditions in the atmosphere or on the surface of the earth, among others, expressed by variables such as temperature, air pressure and wind [2, 5, 6]. However, incomplete understanding of underlying complex atmospheric processes as well as the uncertainties in the initial conditions of the governed differential equation may limit the accuracy of weather forecast to a few days

---

*Authors contributed equally. Names in alphabetical order.
**Corresponding author. S. Mehrkanoon also with Mathematics Centre Maastricht, Maastricht University, The Netherlands
(e-mail: siamak.mehrkanoon@maastrichtuniversity.nl).

[2, 7]. In addition, the computer simulation of NWP requires high computing power and enough time to process [8, 9].

In recent years, machine learning data-driven based models have emerged and proven to significantly reduce the processing time for weather forecasting [8]. Unlike model-driven NWP models, machine learning models make no assumptions about underlying physical factors influencing the weather [8]. They rather rely on large amounts of historical weather observations which are used to extract and learn the relationship between input and output data which then are used to predict future weather conditions [2, 10, 11].

However, the spatiotemporal nature of the underlying time series data, with nonlinear behavior causes the prediction task to be nontrivial [12]. The growing availability of data and advancements in computing power has motivated many researchers to explore a variety of deep learning approaches based on Artificial Neural Networks (ANN) [13]. Especially, Convolutional Neural Networks (CNN) and Recurrent Neural Networks (RNN), such as Long Short Term Memory (LSTM) neural networks, have been successfully used to forecast hourly air temperature with significantly small errors for one time step ahead [7, 14]. In particular, CNNs based models do not require any feature engineering; instead, they rely on feature extraction during the training of the network [3]. Recently the authors in [2] proposed a 3d-CNN based model for temperature forecasting.

The authors in [15] proposed the Dynamic Convolutional Layer for short-range weather prediction task. In particular, in contrast to traditional CNN approaches in Dynamic Convolutional Layer the filters vary from input to input during testing. RNNs, on the other hand, generally perform well when dealing with time-series data [3]. In particular, LSTM networks can better model long-term dependencies [16]. Long- and Short-term Time-series network (LSTNet) [1] leverages both CNN and RNN to extract short-term local dependency patterns among variables and to discover long-term patterns for time series trends. The ConvLSTM network combines both CNN and LSTM architectures for precipitation prediction [17]. However, the sequential nature of processing elements in RNNs limits the parallelization during training, which becomes critical at longer sequence lengths [18].

Vaswani et al. [18] introduced an attention mechanism to model dependencies in sequences regardless of the distances between positions of the input elements. Often such attention mechanisms are combined with RNNs [18]. Temporal pattern attention LSTM (TPA-LSTM) [19] utilizes an attention mechanism that allows the model not only to attend to relevant previous times but also to identify interdependencies among multiple features. The dual-stage attention-based recurrent neural network (DA-RNN) [20] incorporates a dual-stage attention scheme consisting of an encoder with an input attention mechanism and a decoder with a temporal attention mechanism.

2.2. Transformer architecture

The Transformer is an attention-based encoder-decoder architecture that was first introduced in 2017 [18]. It is designed to use the attention mechanism to handle sequential data by processing all input tokens at the same time. It replaces recurrent layers, commonly used in encoder-decoder architectures, with multi-headed self-attention where the dot-product attention is extended with a scaling factor of key-dimension $\frac{1}{\sqrt{d_k}}$ [18]. Consequently, the model does not rely on sequential processing of the data and therefore creates the possibilities for parallelization and reducing the training computational times [18]. Another commonly used attention mechanism is the additive attention, which uses a feed-forward neural network for the computation of the attention [21].

The Transformer is at the heart of many recent breakthroughs and developments in the field of sequence-to-sequence models. It has improved the state-of-the-art in many natural language processing tasks such as machine translation [18], document generation [22] as well as syntactic parsing [23]. The pretrained transformer language models, Bidirectional Encoder Representations from Transformers (BERT) and Generative Pre-trained Transformer (GPT) proved their effectiveness in tasks such as natural language understanding and question answering [24, 25]. Generative models such as the Image Transformer [26] and Music Transformer [27] proved to generate convincingly natural images and musical compositions based on human evaluation.

The authors in [28] used tensorized transformer to compress model parameters and increase performance. In particular, [28] introduced Multi-linear attention for language modeling approaches, which uses Tucker decomposition [29, 30] in Single-block attention to reconstruct the scaled dot-product attention and Block-Term Tensor Decomposition [31] for the multi-head attention mechanism. This paper proposes a Tensorized Encoder Transformer (TENT) for temperature forecasting task. The model is equipped with a new tensorial attention mechanism. As opposed to [28], our proposed TENT model receives 3-dimensional tensors as input and maintains the tensorial format in the calculation of the self-attention layer. Thanks to the introduced tensorial self-attention mechanism, TENT model is able to capture the dependencies between time steps and weather stations. In the subsequent sections, the proposed model will be explained in detail.

3. Proposed Methodology

3.1. Tensorized Encoder Transformer

Here we extend the original Transformer [18] and introduce the Tensorized Encoder Transformer (TENT) model suitable for learning complex underlying patterns of tensorial input data. The model processes inputs of 3D tensorial format $X \in \mathbb{R}^{T \times C \times F}$ where T is the number of time steps, and C and F represent 2D features. 2D features of size $C \times F$ represent a matrix of weather variables such as temperature, humidity and wind speed measured in different geographical locations. For instance different cities along dimension C and weather variables along dimension F. It should be noted that our model can also be used for applications other than weather forecasting, where the input

data has a 3D tensorial format. It is an encoder-only Transformer architecture that consists of a positional encoding layer, three encoder layers followed by a fully-connected layer with linear activation as shown in Fig. 1. Each encoder layer uses the tensorial attention introduced in sections 3.3 and 3.4. Subsequent to the tensorial attention are a residual connection and a normalization layer. After the tensorial attention layer, each head has its own fully connected feed-forward network with two linear transformations and ReLU activations [32], followed by a second residual connection and normalization layer [18].
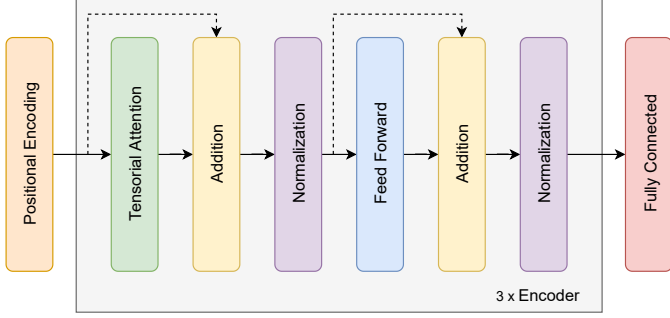

Figure 1: Model architecture of Tensorized Encoder Transformer (TENT).

3.2. Positional Encoding

We use a fixed positional encoding to equip the model with time sequence information. The positional encoding [18] is calculated for the time step T and city C axes according to the Eq. (1), where C is the length of the city axis, pos is the position in time step axis and i is the position in the city axis. We broadcast the values along the weather variables axis F. Hence, the values of the positional encoding are identical across the axis F, and differ in T and C axes.

$$
\begin{cases}
PE_{(pos,2i)} = \sin(pos/10000^{2i/C}), \\
PE_{(pos,2i+1)} = \cos(pos/10000^{2i/C}).
\end{cases} \quad (1)
$$

3.3. Tensorial self-attention

To formulate tensorial self-attention we use the following slice notation. For a tensor $A \in \mathbb{R}^{X \times Y \times Z}$ the x slice is the matrix $(A_{y,z})_x \in \mathbb{R}^{Y \times Z}$ formed from all the values of the A tensor where the first dimension is set to x. Similarly, the x, y slice of A is the vector $(A_z)_{x,y} \in \mathbb{R}^Z$ formed from the values of A where the first and second dimensions are set to x and y respectively. We denote the dimension of the slice by the small letter corresponding to the particular dimension.

The input of the tensorial self-attention is a 3D tensor $X \in \mathbb{R}^{T \times C \times F}$. In the first step of the tensorial self-attention, the 3D tensors Query (Q), Key (K) and Value (V) which all have the same dimension, i.e. $\mathbb{R}^{T \times C \times D}$, are calculated. Here D is obtained by dividing the key-dimension d_k by the number of heads, which are both hyper-parameters.

Three separate 3D weight tensors W^Q, W^K and $W^V \in \mathbb{R}^{C \times F \times D}$ are used. Each t, c slice of Q, K and V (i.e. $(Q_d)_{t,c}$, $(K_d)_{t,c}$ and $(V_d)_{t,c}$ respectively) is calculated by multiplying the t, c slice of X, notated as $(X_f)_{t,c}$, and the c slice of W^Q, W^K and

W^V (i.e. $(W^Q_{f,d})_c$, $(W^K_{f,d})_c$ and $(W^V_{f,d})_c$ respectively) as shown in Eq. (2)-(3). Fig. 2 illustrates the visualization of the abovementioned steps.

$$(Q_d)_{t,c} = (X_f)_{t,c} \times (W^Q_{f,d})_c \quad \forall t = 1, \ldots, T, \quad c = 1, \ldots, C. \quad (2)$$

$$(K_d)_{t,c} = (X_f)_{t,c} \times (W^K_{f,d})_c \quad \forall t = 1, \ldots, T, \quad c = 1, \ldots, C. \quad (3)$$

$$(V_d)_{t,c} = (X_f)_{t,c} \times (W^V_{f,d})_c \quad \forall t = 1, \ldots, T, \quad c = 1, \ldots, C. \quad (4)$$
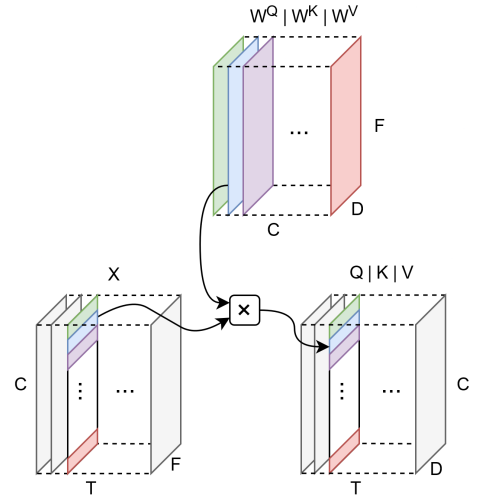

Figure 2: Visualization of the slice multiplication for obtaining query, key and value matrices from the input X and weight matrices W^Q, W^K and W^V. In this figure, slices in the input are multiplied by the slices of weight matrices of the same color to form a slice of that color in the output tensors Q, K, and V.

In the next step, each time step t slice of Q (notated as $(Q_{c,d})_t$) is multiplied with each time step t' transposed slice of K (notated as $((K_{c',d})_{t'})^T$). All multiplications result in matrices of shape $C \times C'$, which are slices of a tensor $\tilde{R} \in \mathbb{R}^{T \times T' \times C \times C'}$, where T and C are the first and second dimensions of Q tensor and T' and C' are the first and second dimensions of K tensor. $\tilde{R}$ tensor is in turn summed over the last dimension and divided element-wise by the square root of D (following the formulation in [18]) producing a tensor $R \in \mathbb{R}^{T \times T' \times C}$. The entire calculation is shown in Eq. (5).

$$
\begin{aligned}
(\tilde{R}_{c,c'})_{t,t'} &= (Q_{c,d})_t \times ((K_{c',d})_{t'})^T \quad \forall t, t' = 1, \ldots, T, \\
R &= \frac{1}{\sqrt{D}} \sum_{c'=1}^{C} (\tilde{R}_{t,t',c})_{c'}.
\end{aligned} \quad (5)
$$

Next, we apply a softmax function over each t, t' slice of R, producing attention scores $S \in \mathbb{R}^{T \times T' \times C}$ as follows:

$$(S_c)_{t,t'} = \text{softmax}((R_c)_{t,t'}) \quad \forall t, t' = 1, \ldots, T. \quad (6)$$

3

Lastly, the output tensor $Z \in \mathbb{R}^{T \times C \times D}$ is calculated by taking the Hadamard product from the t, t' slice of the attention weights $(S_c)_{t,t'}$ and the t' slice of V (i.e. $(V_{c,d})_{t'}$), and summing over the second dimension (corresponding to t'). One should note that $(S_c)_{t,t'}$ slice is broadcasted to shape $C \times D$ to match the shape of $(V_{c,d})_{t'}$ slice. This calculation can be seen in Eq. (7).

$$(Z_{c,d})_t = \sum_{t'=1}^{T} (S_c)_{t,t'} \circ (V_{c,d})_{t'} \quad \forall t = 1, \ldots, T. \quad (7)$$

3.4. Tensorial multihead-attention

In this work, we use multiple heads to calculate the tensorial self-attention multiple times over the dataset. To this end, we modify the calculation of the multihead attention [18] to tensorial inputs. Each of these heads correspond to the output of the tensorial self-attention. The outputs are concatenated in the last dimension and each time slice is multiplied with a time slice of a weights tensor with shape $T \times (H \cdot D) \times F$, which leads to an output tensor $Y \in \mathbb{R}^{T \times C \times F}$ as shown in Eq. (8),

$$(Y_{c,f})_t = (\mathbin{\|}_{h=1}^{H} (Z_h)_{c,h \cdot d})_t \times (W_{h \cdot d, f}^o)_t \quad \forall t = 1, \ldots, T, \quad (8)$$

where $\|$ represents concatenation.

3.5. Attention Scores

We use attention scores calculated from the attention weights to explain our model. The attention weights have been previously used for feature selection purposes [33], as well as explainability [34]. We extract the weights in the first layer after the softmax shown in Fig. 3. The extracted weights are denoted by $S \in \mathbb{R}^{H \times T_q \times T_k \times C}$, where H is the number of heads, T_q and T_k are the numbers of time steps due to the Query and the Key respectively and C is the number of cities.

In order to show the correlation between heads and cities, the attention score s_{hc} is computed as follows:

$$s_{hc} = \sum_{t=1}^{T_q} \sum_{t'=1}^{T_k} s_{t,t'} \quad \forall h = 1, \ldots, H, \quad c = 1, \ldots, C. \quad (9)$$
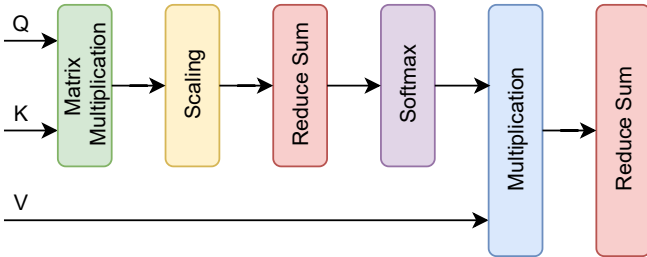

Figure 3: Tensorial self-attention.

Furthermore, in order to show the contribution of each city to the prediction, we calculate the attention score s_c for each city as follows:

$$s_c = \sum_{h=1}^{H} s_{hc} \quad \forall c = 1, \ldots, C. \quad (10)$$

4. Experiments

We apply our proposed TENT model on two datasets and compare the obtained results with two other models - encoder part of the original Transformer [18] (with the input tensor flattened) and 3d-CNN [2]. Following the lines of [2, 8], the Mean Absolute Error (MAE) and Mean Squared Error (MSE) metrics are used to evaluate the performance of the models as follows:

$$\text{MAE} = \frac{\sum_{i=1}^{n} |y_i - \hat{y}_i|}{n}, \quad \text{MSE} = \frac{\sum_{i=1}^{n} (y_i - \hat{y}_i)^2}{n}. \quad (11)$$

Here, n is the number of samples, $\hat{y}_i$ is the model prediction and y_i is the true measurement. The training is done with MSE loss function for a maximum of 300 epochs, and early stopping based on validation loss with patience 20 is used. Batch size is set to 128, and Adam optimizer [35] is employed. Both TENT and Transformer use custom learning rate schedule [18] while 3d-CNN uses a learning rate adapted by Adam optimizer. The optimal hyper-parameters for each model that were found empirically can be seen in Table 1.

Table 1: Hyper-parameters used for all the experiments for the two datasets. The parameters of Transformer and 3d-CNN models for two datasets are the same.

Model	Hyper-parameter	USA/Canada	Europe
TENT	Layer Number	3	3
	Head Number	32	128
	Key-Dimension	256	3072
	Dense Units	128	128
Transformer	Layer Number	3	
	Head Number	16	
	Key-Dimension	1024	
	Dense Units	1024	
3d-CNN	Filters	10	
	Kernel Size	2	
	Dense Units	158	
	Learning Rate	10^{-4}	

4.1. Dataset USA and Canada

The first dataset[1] contains hourly measurements of the weather attributes such as humidity, air pressure, temperature, weather description, wind direction and wind speed for 30 cities in USA and Canada from October 2012 to November 2017.
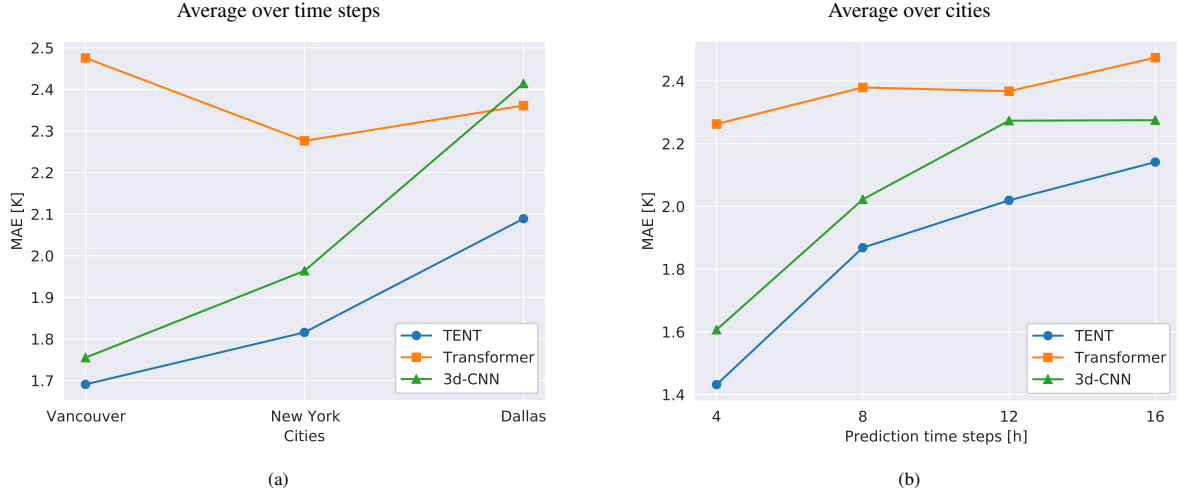
---

[1] https://surfdrive.surf.nl/files/index.php/s/LemhAC362d8FU5s

4

(a)

(b)

Figure 4: The obtained test MAE of the models for the **USA and Canada** dataset averaged over cities (4a) and prediction time steps (4b).

Table 2: The obtained test MAE and MSE of the **USA and Canada** dataset for predicting temperature.

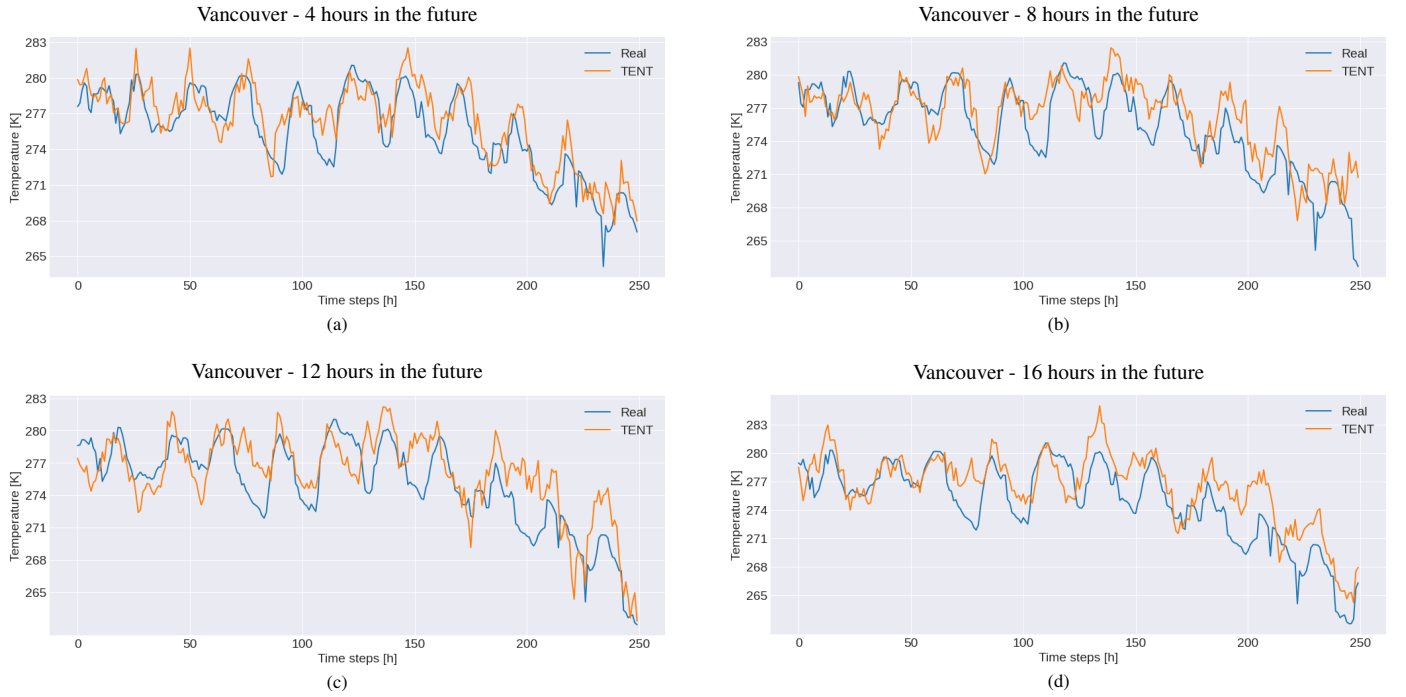| Station	Model	MAE				MSE			
		4 hours	8 hours	12 hours	16 hours	4 hours	8 hours	12 hours	16 hours
	TENT	**1.352**	**1.688**	**1.810**	1.913	**3.108**	**4.740**	**5.479**	6.059
Vancouver	Transformer	2.515	2.553	2.392	2.442	11.62	11.67	10.14	10.66
	3d CNN	1.486	1.855	1.856	**1.823**	3.650	5.688	5.744	**5.520**
	TENT	**1.370**	**1.825**	**1.980**	**2.088**	**3.145**	**5.581**	**6.578**	**7.330**
New York	Transformer	2.089	2.252	2.293	2.471	7.017	8.371	8.653	9.952
	3d CNN	1.499	1.896	2.131	2.329	3.704	5.950	7.455	8.879
	TENT	**1.573**	**2.092**	**2.268**	**2.423**	**4.378**	**7.865**	**9.022**	**10.21**
Dallas	Transformer	2.184	2.333	2.417	2.510	8.045	9.190	9.702	10.58
	3d CNN	1.835	2.316	2.833	2.673	5.587	9.159	13.46	11.96

(a)

(b)

(c)

(d)

Figure 5: The comparison between the predictions of TENT model and the real measurements for **hourly temperature** of the test set of **Vancouver**.

5

Table 3: The obtained test MAE and MSE of the **Europe** dataset experiments for predicting temperature.

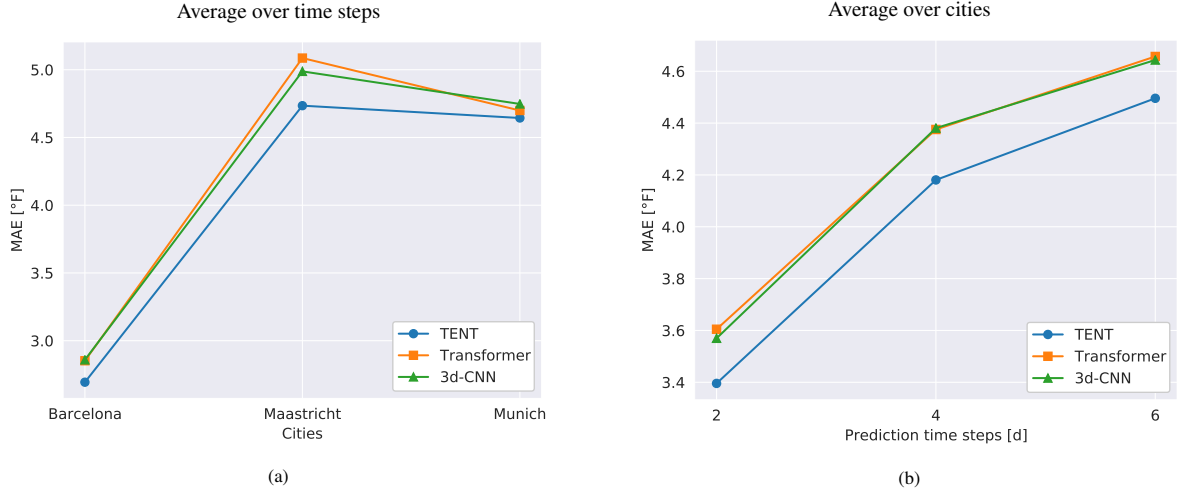| Station	Model	MAE			MSE		
		2 days	4 days	6 days	2 days	4 days	6 days
Barcelona	TENT	**2.327**	**2.807**	**2.947**	**9.533**	**13.79**	**15.14**
	Transformer	2.608	2.901	3.047	11.70	14.66	15.92
	3d CNN	2.502	3.015	3.059	10.73	14.64	15.74
Maastricht	TENT	**4.164**	**4.900**	**5.140**	**28.45**	**38.50**	**42.70**
	Transformer	4.370	5.239	5.649	30.89	43.23	50.67
	3d CNN	4.276	5.078	5.609	28.82	40.51	49.41
Munich	TENT	**3.696**	**4.835**	5.400	**21.97**	**36.04**	45.30
	Transformer	3.836	4.986	5.275	23.94	39.05	43.56
	3d CNN	3.931	5.049	**5.262**	24.87	39.57	**43.50**

Figure 6: The obtained test MAE of the models for the **Europe** dataset averaged over cities (6a) and prediction time steps (6b).

The longitude and latitude information of the cities are converted to Cartesian coordinates which, in turn, are used in normalized form as three additional features [36, 37] as follows:

$$\begin{cases} x = \cos(\phi) \cdot \cos(\lambda), \\ y = \cos(\phi) \cdot \sin(\lambda), \\ z = \sin(\phi). \end{cases} \quad (12)$$

where ϕ and λ are the latitude and longitude, respectively. Due to the time periodicity in the dataset, the day of the year and the hour of the day are added to each sample in the dataset and normalized along with the measurements in the dataset as in Eq. 13 [2]. The data from 2012-2016 is used as a training and validation set and the data from 2016-2017 forms the test set.

$$x_{scaled} = \frac{x - \min(x)}{\max(x) - \min(x)}. \quad (13)$$

We cast the input data to a tensor with the shape $T \times C \times F$, where the first dimension, second and third dimensions represent the time sequence, the cities and the features of the cities respectively.

Predictions are made for 4, 8, 12 and 16 hours into the future (prediction time step) using a lag of 16 hours. In our conducted experiments the lag of 16 hours empirically found to be optimal in terms of a mean prediction error on the validation set. For

this dataset, the target cities are Vancouver, Dallas and New York and the target feature is temperature. The obtained MAEs and MSEs are tabulated in Table 2. Fig. 4 (a) and (b) show averaged MAE over cities and time steps, respectively. A subset of the obtained prediction and real measurement for the city of Vancouver, having 4, 8, 12 and 16 as prediction time step, are depicted in Fig. 5.

4.2. Dataset Europe

The second dataset[1] contains daily measurements of the weather attributes of 18 cities across Europe from May 2005 to April 2020. The time periodicity is added in the form of the day of the year and normalized as other features. The data from 2005-2017 is used for training and validation and the data from 2017-2020 is used as the test set.

In this dataset, we perform experiments for 2, 4 and 6 days ahead prediction. The optimal lag parameter used to construct the regressor is empirically found and is set to 8 days. The target cities are Barcelona, Maastricht and Munich and the target feature is the average temperature. The obtained MAEs and MSEs are tabulated in Table 3. Fig. 6 (a) and (b) shows the MAE of the models averaged over cities and prediction time steps respectively. Furthermore, Fig. 7 shows the model prediction and the real measurements of a subset of our test set for
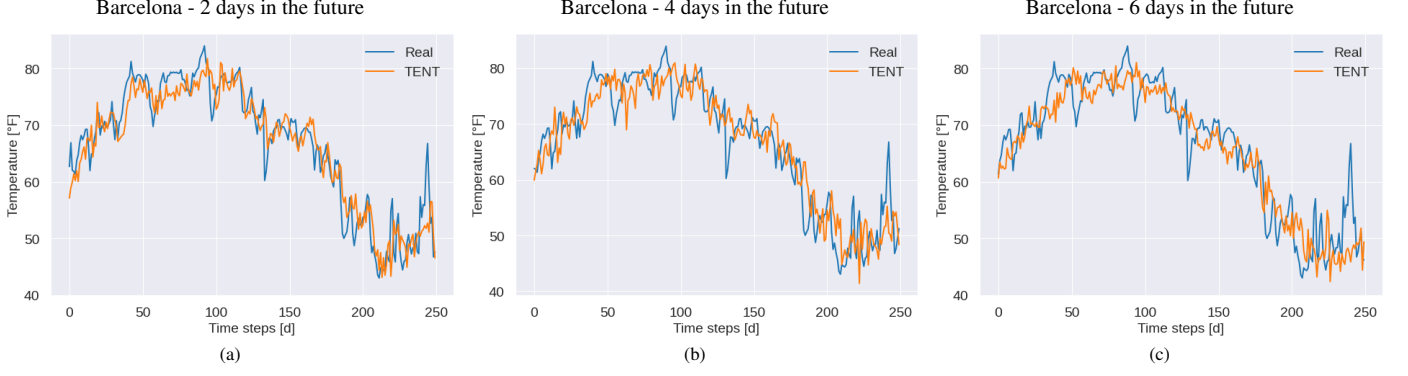
Figure 7: The comparison between the predictions of TENT model and the real measurements for **average daily temperature** of the test set of **Barcelona**.
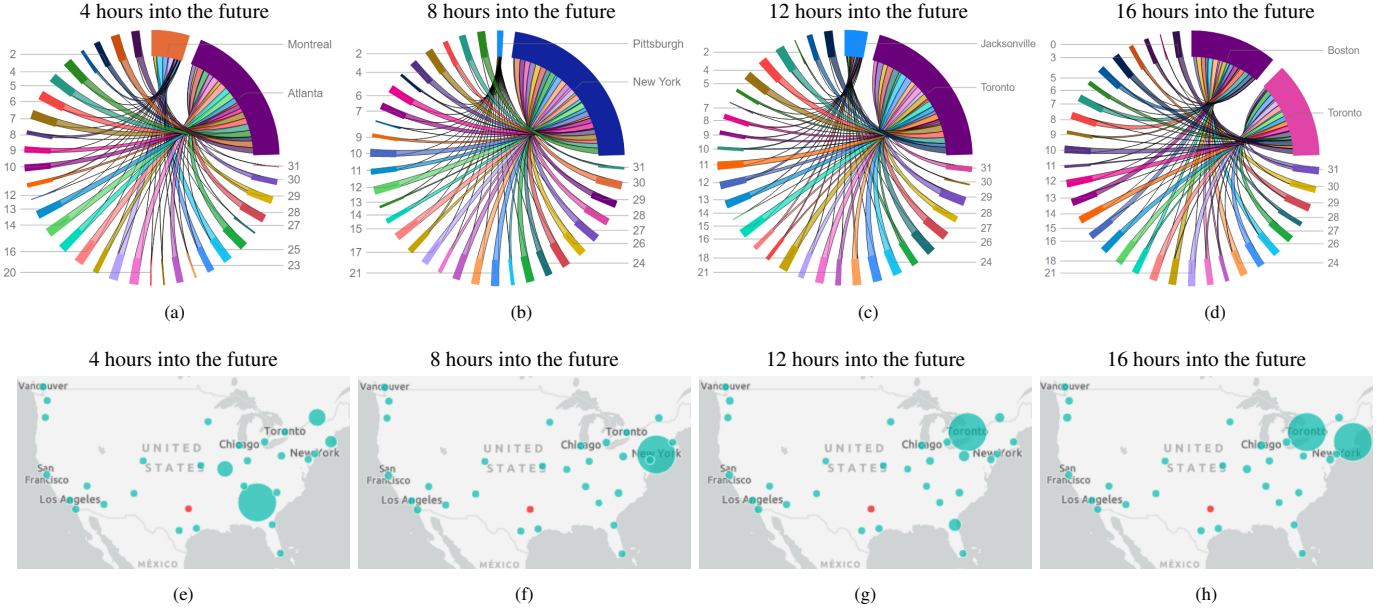

Figure 8: Attention scores for **Dallas** in USA and Canada dataset. The top graphs show which city each of the heads attends to. The thickness of the line represents the amount of attention each of the heads is paying to the cities.

the city of Barcelona 2, 4 and 6 days into the future.

5. Discussion

In the USA and Canada dataset experiments, MAE and MSE results exhibit consistent pattern, with the TENT model performing better than other tested models almost for all tested time step ahead predictions. Our model also exhibited the lowest average MAE and MSE over cities and prediction time steps.

Although Transformer performed worse than other models on Vancouver and New York predictions, it achieved smaller error than 3d-CNN on 12 and 16 hours ahead predictions in Dallas. The obtained results of the Europe dataset experiments are similar to those of the previous dataset, i.e. TENT almost in all prediction steps outperforms the other tested models, and average errors are smaller for both cities and prediction time steps.

In what follows, we use the attention score s_{hc} in Eq. (9) to show to which city each of the heads is paying attention to when predicting the output of the model. In particular, the analysis

is provided for three target cities, i.e. Dallas, Vancouver and Munich in Figs. 8, 9 and 10 respectively. In addition, in order to quantify the contribution of each city to the target city we use the attention score obtained from Eq. (10). The visualization of the attention scores for the above-mentioned target cities are shown in Figs. 8 (a-d) and 9 (a-d) and 10 (a-c).

In these plots, e.g. 8 (a-d), one can see the name of cities and numbers, the latter represents each of the heads used in the Tensorial multihead-attention. The thickness of the connecting lines represents the amount of attention that each head gives to the city it is connected to. For the purpose of readability of the plots, we only keep the cities that receive the most attention and the heads that contributed to those cities.

In Figs 8 (e-h), e.g. the size of the circles indicates the importance of each city in the temperature prediction for the target city. The target city is shown as a red circle. It can be seen that the farther away we are predicting into the future, the distance between the target city and the most important cities for the prediction also increases.

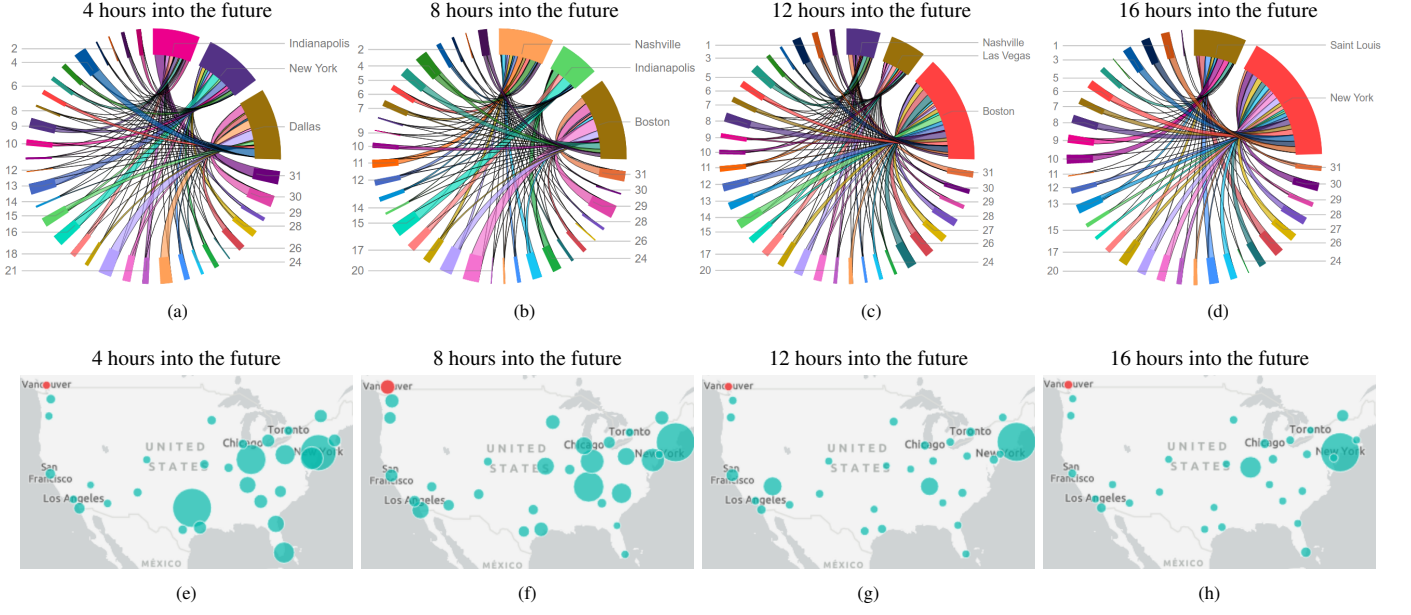Fig. 9 shows the visualization corresponding to the temper-

Figure 9: Attention scores for **Vancouver** in USA and Canada dataset. The top graphs show which city each of the heads attends to. The thickness of the line represents the amount of attention each of the heads is paying to the cities.
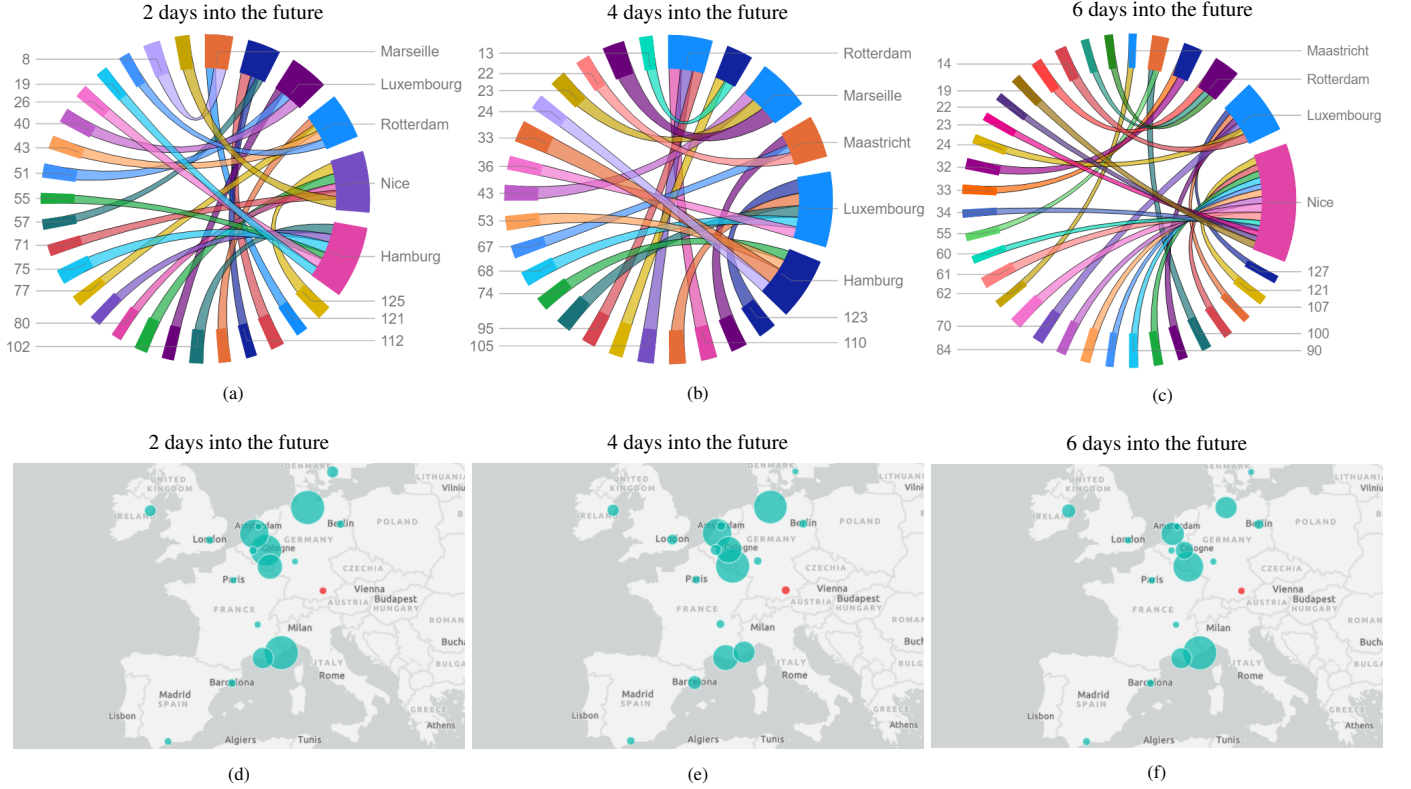

Figure 10: Attention scores for **Munich** in Europe dataset. The top graphs show which city each of the heads attends to. The thickness of the line represents the amount of attention each of the heads is paying to the cities.

ature prediction of Vancouver. In general, similar patterns have been observed, particularly for 12 and 16 hours into the future.

The same representation was made for the Europe dataset. In this dataset, we trained the model instead of hourly temperature measurements on daily average temperature for 2, 4, and 6 days into the future as seen in Tab. 3. The plots of both the

circular graphs and maps, for the city of Munich, can be seen in Fig. 10. Here, it is not possible to observe the same pattern as we observed for the US and Canada dataset, but it can be seen that some of the cities have very little contribution to any of the predictions for Munich, pointing out to possible feature selection by the model.

8

In Figs. 8, 9 and 10, the attention scores that generated both the map and the circular graph are the same for each of the prediction time steps.

6. Conclusion

In this paper, we introduced TENT, a novel transformer based model, for temperature prediction task. Our proposed model outperforms the other examined models for most of the prediction time steps and cities on two real life weather datasets, i.e USA and Canada dataset as well as Europe dataset. In addition, we visualized the feature selection of the tensorial attention, the attention scores for selected cities. From a spatiotemporal perspective, the attention mechanism selects more distant cities with increasing prediction time steps. The introduced model can potentially be used for other applications with 3D tensor inputs and our code[2] is available online.

References

[1] G. Lai, W.-C. Chang, Y. Yang, and H. Liu, "Modeling long-and short-term temporal patterns with deep neural networks," in *The 41st International ACM SIGIR Conference on Research & Development in Information Retrieval*, 2018, pp. 95–104.

[2] S. Mehrkanoon, "Deep shared representation learning for weather elements forecasting," *Knowledge-Based Systems*, vol. 179, pp. 120–128, 2019.

[3] D. Kreuzer, M. Munz, and S. Schlüter, "Short-term temperature forecasts using a convolutional neural network—an application to different weather stations in germany," *Machine Learning with Applications*, vol. 2, p. 100007, 2020.

[4] S. K. Ahmad and F. Hossain, "Maximizing energy production from hydropower dams using short-term weather forecasts," *Renewable Energy*, vol. 146, pp. 1560–1577, 2020.

[5] G. Marchuk, *Numerical methods in weather prediction*. Elsevier, 2012.

[6] L. F. Richardson, *Weather prediction by numerical process*. Cambridge university press, 2007.

[7] S. S. Soman, H. Zareipour, O. Malik, and P. Mandal, "A review of wind power and wind speed forecasting methods with different time horizons," in *North American Power Symposium 2010*. IEEE, 2010, pp. 1–8.

[8] K. Trebing and S. Mehrkanoon, "Wind speed prediction using multidimensional convolutional neural networks," *arXiv preprint arXiv:2007.12567*, 2020.

[9] P. Bauer, A. Thorpe, and G. Brunet, "The quiet revolution of numerical weather prediction," *Nature*, vol. 525, no. 7567, pp. 47–55, 2015.

[10] L. Chen and X. Lai, "Comparison between arima and ann models used in short-term wind speed forecasting," in *2011 Asia-Pacific Power and Energy Engineering Conference*. IEEE, 2011, pp. 1–4.

[11] R. J. Kuligowski and A. P. Barros, "Localized precipitation forecasts from a numerical weather prediction model using artificial neural networks," *Weather and forecasting*, vol. 13, no. 4, pp. 1194–1204, 1998.

[12] I. Bartos and I. M. Jánosi, "Nonlinear correlations of daily temperature records over land," *Nonlinear Processes in Geophysics*, vol. 13, no. 5, pp. 571–576, 2006.

[13] A. G. Salman, B. Kanigoro, and Y. Heryadi, "Weather forecasting using deep learning techniques," in *2015 International Conference on Advanced Computer Science and Information Systems (ICACSIS)*. IEEE, 2015, pp. 281–285.

[14] J. Cifuentes, G. Marulanda, A. Bello, and J. Reneses, "Air temperature forecasting using machine learning techniques: a review," *Energies*, vol. 13, no. 16, p. 4215, 2020.

[15] B. Klein, L. Wolf, and Y. Afek, "A dynamic convolutional layer for short range weather prediction," in *Proceedings of the IEEE Conference on Computer Vision and Pattern Recognition*, 2015, pp. 4840–4848.

[16] S. Hochreiter and J. Schmidhuber, "Long short-term memory," *Neural computation*, vol. 9, no. 8, pp. 1735–1780, 1997.

[17] X. Shi, Z. Chen, H. Wang, D.-Y. Yeung, W.-K. Wong, and W.-c. Woo, "Convolutional lstm network: A machine learning approach for precipitation nowcasting," *arXiv preprint arXiv:1506.04214*, 2015.

[18] A. Vaswani, N. Shazeer, N. Parmar, J. Uszkoreit, L. Jones, A. N. Gomez, Ł. Kaiser, and I. Polosukhin, "Attention is all you need," in *Advances in neural information processing systems*, 2017, pp. 5998–6008.

[19] S.-Y. Shih, F.-K. Sun, and H.-y. Lee, "Temporal pattern attention for multivariate time series forecasting," *Machine Learning*, vol. 108, no. 8-9, pp. 1421–1441, 2019.

[20] Y. Qin, D. Song, H. Chen, W. Cheng, G. Jiang, and G. Cottrell, "A dual-stage attention-based recurrent neural network for time series prediction," *arXiv preprint arXiv:1704.02971*, 2017.

[21] D. Bahdanau, K. Cho, and Y. Bengio, "Neural machine translation by jointly learning to align and translate," *arXiv preprint arXiv:1409.0473*, 2014.

[22] P. J. Liu, M. Saleh, E. Pot, B. Goodrich, R. Sepassi, L. Kaiser, and N. Shazeer, "Generating wikipedia by summarizing long sequences," *arXiv preprint arXiv:1801.10198*, 2018.

[23] N. Kitaev and D. Klein, "Constituency parsing with a self-attentive encoder," *arXiv preprint arXiv:1805.01052*, 2018.

[24] J. Devlin, M.-W. Chang, K. Lee, and K. Toutanova, "Bert: Pre-training of deep bidirectional transformers for language understanding," *arXiv preprint arXiv:1810.04805*, 2018.

[25] A. Radford, K. Narasimhan, T. Salimans, and I. Sutskever, "Improving language understanding with unsupervised learning," *Technical report, OpenAI*, 2018.

[26] N. Parmar, A. Vaswani, J. Uszkoreit, Ł. Kaiser, N. Shazeer, A. Ku, and D. Tran, "Image transformer," *arXiv preprint arXiv:1802.05751*, 2018.

[27] C.-Z. A. Huang, A. Vaswani, J. Uszkoreit, N. Shazeer, I. Simon, C. Hawthorne, A. M. Dai, M. D. Hoffman, M. Dinculescu, and D. Eck, "Music transformer," *arXiv preprint arXiv:1809.04281*, 2018.

[28] X. Ma, P. Zhang, S. Zhang, N. Duan, Y. Hou, D. Song, and M. Zhou, "A tensorized transformer for language modeling," 2019.

[29] L. R. Tucker, "Some mathematical notes on three-mode factor analysis," *Psychometrika*, vol. 31, no. 3, pp. 279–311, 1966.

[30] G. Li, J. Ye, H. Yang, D. Chen, S. Yan, and Z. Xu, "Bt-nets: Simplifying deep neural networks via block term decomposition," *arXiv preprint arXiv:1712.05689*, 2017.

[31] L. De Lathauwer, "Decompositions of a higher-order tensor in block terms—part ii: Definitions and uniqueness," *SIAM Journal on Matrix Analysis and Applications*, vol. 30, no. 3, pp. 1033–1066, 2008.

[32] V. Nair and G. E. Hinton, "Rectified linear units improve restricted boltzmann machines," in *ICML*, 2010, pp. 807–814.

[33] N. Gui, D. Ge, and Z. Hu, "Afs: An attention-based mechanism for supervised feature selection," *Proceedings of the AAAI Conference on Artificial Intelligence*, vol. 33, no. 01, pp. 3705–3713, Jul. 2019. [Online]. Available: https://ojs.aaai.org/index.php/AAAI/article/view/4255

[34] S. Wiegreffe and Y. Pinter, "Attention is not not explanation," *arXiv preprint arXiv:1908.04626*, 2019.

[35] D. P. Kingma and J. Ba, "Adam: A method for stochastic optimization," *arXiv preprint arXiv:1412.6980*, 2014.

[36] S. J. Claessens, "Efficient transformation from cartesian to geodetic coordinates," *Computers & Geosciences*, vol. 133, p. 104307, 2019.

[37] B. Hofmann-Wellenhof and H. Moritz, *Physical geodesy*. Springer Science & Business Media, 2006.

---

[2]https://github.com/onurbil/TENT